JOURNAL OF CHEMICAL & ENGINEERING DATA

ARTICLE

pubs.acs.org/jced

Adsorption and Diffusion of Ethyl Acetate on the Chromium-Based Metal−Organic Framework MIL-101

Jiao Shi, Zhenxia Zhao, Qibin Xia, Yingwei Li, and Zhong Li*

School of Chemistry and Chemical Engineering and State Key Laboratory of Subtropical Building Science, South China University of Technology, Guangzhou, 510640, P. R. China

ABSTRACT: The adsorption equilibrium and diffusion of ethyl acetate (EA) on chromium-terphthalate-based crystals (MIL-101) are experimentally studied. The MIL-101 synthesized in this work shows an extra-high surface area of 5014 $m^2 \cdot g^{-1}$ (Langmuir). Adsorption isotherms and kinetic curves of EA on the MIL-101 are measured by a gravimetric method. Results show that the isotherms of EA can be fitted favorably by the Langmuir equation. The adsorption capacity of the MIL-101 for EA is up to 10.5 $mmol \cdot g^{-1}$ at 288 K and 54 mbar. Diffusion coefficients of EA within the MIL-101 are in the range of (1.617 to 2.264) $\cdot 10^{-10}$ $cm^2 \cdot s^{-1}$ in (288 to 318) K with a lower activation energy of 8.361 $kJ \cdot mol^{-1}$. The isosteric heat of EA adsorption on the MIL-101 is within the range of (36.48 to 42.25) $kJ \cdot mol^{-1}$. The isosteric adsorption heat increased slightly with the amount adsorbed of EA, implying the existence of favorable lateral interactions between EA molecules. Multiple adsorption−desorption cycles are conducted at 298 K to examine the reversibility of EA adsorption on the MIL-101. Adsorptions were performed separately at (2, 3, 5, 7, and 10) mbar, and desorptions are performed at 0.05 mbar. Experimental results show that the EA adsorption on the MIL-101 is highly reversible and the desorption efficiency of EA is up to 98.4 %.

1. INTRODUCTION

Volatile organic compounds (VOCs) are a large group of chemicals having vapor pressures greater than 133.3 Pa at room temperature and being easily vaporized at ambient temperature and pressure. As important sources of air pollutants, most of VOCs are emitted from various industrial processes that manufacture or utilize organic solvents. Ethyl acetate,[1] EA for short, is just among those typical industrial solvents, which is widely used in petrochemical, pharmaceutical, coating, color printing, synthetic fiber, and polymer industries. It has been pointed out that the long-term exposure to EA as well as other VOCs, even with very low concentrations, can cause adverse effect or damage for human beings. Given the increased concern of the health hazard associated with VOCs, the research on the abatement of VOCs has been attracting unabated attention. Adsorption is generally considered to be a safe and economically feasible method for removing VOCs with low concentrations or trace amounts.[2,3] One decisive aspect for the efficiency of adsorption is the property of adsorbents. Nowadays, the most widely used adsorbents for VOCs adsorption were activated carbon, zeolites, molecular sieves, and adsorptive resins.

Wang et al.[4] measured the adsorption of six different acetate compounds on activated carbon, silica gel, and 13X zeolite and reported that activated carbon had the highest adsorption capacity for EA. It was also found that the acquired equilibrium isotherm data were well-fitted by both the Freundlich and Langmuir equations in the acceptable deviations. Manjare and Ghoshal[5−7] studied the adsorption amounts of EA on activated carbon and two different zeolites (5A and 13X). Their experimental results showed that the adsorption capacity of three adsorbents were in the order of activated carbon >13X > 5A, and the isotherms of EA on all adsorbents were of type I which were well-depicted by the Langmuir isotherms. Studies of the adsorption of EA on other materials were also reported. Cavazzini et al.[8] measured the adsorption equilibria of EA on a polysaccharide-based adsorbent and reported that EA adsorption could be modeled by a Bi-Langmuir isotherm model. Li et al.[9] studied the adsorption property of semicoke for EA. They reported that the amount adsorbed of EA on the semicoke was higher than that of benzene, and the extended Langmuir equation agreed well with the experimental isotherm data of EA.

Recently, the development of a new class of nanoporous materials known as metal−organic frameworks (MOFs) provides alternative adsorbents for an adsorption technique. MOFs are representative of novel crystalline porous materials hybridized with transition ions and organic linkers, which possess a wide range of properties including extra-high specific surface area, ordered porous structure, and adjustable chemical functionality. These properties have made them potential candidates to be applied in various fields such as gas storage and gas adsorption/separation. MIL-101, a porous chromium-terphthalate-based solid,[10] is one of the most prominent examples among many MOFs that have been studied. It exhibits not only huge BET and Langmuir surface areas (4100 ± 200 $m^2 \cdot g^{-1}$; 5900 ± 200 $m^2 \cdot g^{-1}$), a giant cell volume (702 000 $Å^3$), but also an ordered mesoporous zeotype architecture with a MTN topology. Besides, MIL-101 also shows a high hydrothermal stability,[11] which along with its high porosity makes MIL-101 a promising adsorbent. The adsorption properties of MIL-101 for several gases and organic vapors have been studied. Ferey et al.[12] measured high pressure CO_2 and CH_4 adsorption on the MIL-101 at 303 K and

Received: April 29, 2011
Accepted: July 11, 2011
Published: July 22, 2011

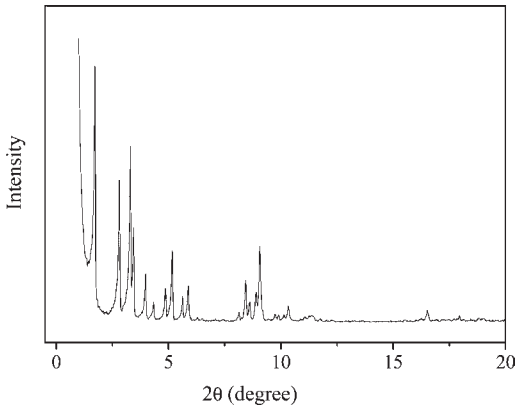

Figure 1. XRD pattern of the MIL-101 synthesized by using the hydrothermal method.

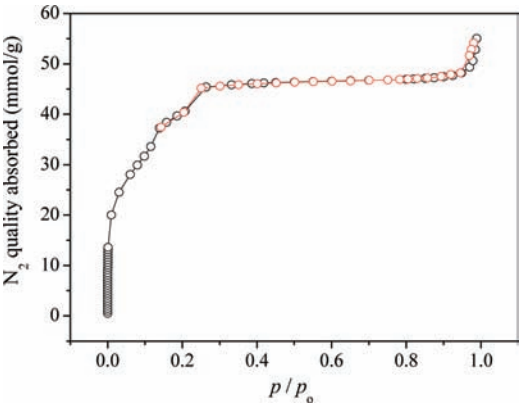

Figure 2. Nitrogen sorption isotherms at 77 K of the MIL-101 synthesized in this work. p/p_o is the ratio of gas pressure (p) to saturation pressure (p_o = 760 Torr).

reported high uptakes of both CO_2 (40 mmol·g^{-1} at 5 MPa) and CH_4 (13.6 mmol·g^{-1} at 6 MPa). They also investigated the adsorption of H_2S on the MIL-101 at room temperature and concluded that MIL-101 could be stable and easily regenerable toward H_2S sorption.[13] Zhao et al.[14] studied the adsorption equilibrium and diffusion kinetics of benzene on the MIL-101. They reported that MIL-101 had a huge adsorption capacity for benzene (16.5 mmol·g^{-1} at 288 K and 56.0 mbar), and benzene diffusion within the MIL-101 crystals is an activated process with diffusivity in the range of (4.25 to 4.67)·10^{-9} cm^2·s^{-1} at (288 to 318) K. However, up to now, no experiment has been conducted to investigate the adsorption of EA on the MIL-101.

The objective of this paper is to study the adsorption equilibrium and diffusion kinetics of EA on the MIL-101 by a gravimetric method. A suitable adsorption isotherm representing the equilibrium data of EA on the MIL-101 was proposed. The diffusion coefficient of EA within the MIL-101 was calculated on the basis of kinetic data of EA adsorption. The activation energy of adsorption as well as the isosteric heat of adsorption for EA on the MIL-101 would be also estimated and reported here. To examine the reversibility of EA adsorption on the MIL-101, consecutive adsorption−desorption cycles were performed and reported.

2. EXPERIMENTAL SECTION

2.1. Materials. Chromium(III) nitrate nonahydrate ($Cr(NO_3)_3·9H_2O$, > 98.5 % purification) was purchased from Alfa Aesar; 1,4-benzene dicarboxylic acid (H_2BDC, ≥ 99.0 % purity) was purchased from Acros Organic, and hydrofluoric acid (HF, ≥ 40.0 % purity) was purchased from Guangzhou Chemical Reagent Factory, which were used as received from vendors without further purification.

2.2. Synthesis of MIL-101. The chromium terephthalate MIL-101 was synthesized using hydrothermal method, and the original steps were already reported elsewhere.[10] First, the reactant mixture with a molar composition of 1 $Cr(NO_3)_3·9H_2O$: 1 H_2BDC: 1 HF: 278 H_2O was loaded into a Teflon-lined stainless steel reactor and then sealed. Then, the reactor was placed in an autoclave (CWF 1300, Carnolite) at 493 K and held for 8 h. After the reaction time, the reactor was gradually cooled down to the room temperature. Fine green colored powders were obtained as the major product, while a significant amount of recrystallized H_2BDC could be found. To acquire pure crystalline material with high porosity and surface area, a series of purification similar with the reported method[15] were applied to remove the nonreacted H_2BDC as well as other guest molecules in the sample. The procedure of purification was mainly comprised with two consecutive solvent treatments using *N*,*N*-dimethylformamide (DMF, > 99 %, from Mallinckrodt) and hot ethanol solution (> 99.7, from Tianjin Fuyu) separately. After that, the product was dried at 423 K overnight. Finally, the crystalline material of MIL-101 was obtained. The particle size of the sample was measured by using Malvern Mastersizer 2000 laser size analyzer. The average particle radius (r_c) of the sample was 10 μm.

2.3. Adsorbent Characterization. The powder X-ray diffraction (XRD) patterns of the as-synthesized MIL-101 sample was determined by a D/max-IIIA diffractometer (Rigaku Co., Japan) operating at 35 kV and 25 mA by using Cu Kα1 radiation (λ = 1.54056). Nitrogen adsorption and desorption isotherms were measured by a Micromeritics ASAP 2010 adsorption porosimeter at a liquid nitrogen temperature of 77 K after being degassed under vacuum at 423 K for 5 h. The specific surface areas were calculated using the Langmuir and Brunauer−Emmett−Teller (BET) methods, and the pore size distribution curve was calculated by the density functional theory (DFT). The pore volume was taken by a single point method at p/p_0 = 0.978.

2.4. EA Vapor Adsorption Experiments. The adsorption experiments were performed using the intelligent gravimetric analyzer (IGA-003, Hiden), which allows isotherms and corresponding kinetics of the adsorption and desorption to be determined for set pressure steps. In IGA-003, an ultrasensitive microbalance of resolution 0.2 μg is mounted in the thermostatted heatsink with high precision temperature control. The sample was weighed about (56 to 59) mg for each run. Before the measurements, the sample in the vessel of IGA-003 was vacuumed up to (3 to 5) Pa and outgassed at 423 K for 5 h. The measurements were performed separately at three different temperatures (288 K, 298 K, and 308 K) in terms of the built-in water baths. The amounts adsorbed of EA on the MIL-101 sample can be calculated as follows:

$$Q_e = \frac{1000(W_e - W_a)}{W_a M_{EA}} \quad (1)$$

$$Q_t = \frac{1000(W_t - W_a)}{W_a M_{EA}} \quad (2)$$

dx.doi.org/10.1021/je2004098 |*J. Chem. Eng. Data* 2011, 56, 3419–3425

Table 1. Pore Structure Parameters of the MIL-101 Samples Cited in Different References

	BET	Langmuir	pore volume		
method	$m^2 \cdot g^{-1}$	$m^2 \cdot g^{-1}$	$cm^3 \cdot g^{-1}$	researcher	reference
hydrothermal	3446	5014	1.75		present work
hydrothermal		4500−5500	1.5−1.9	Ferey et al.	10
hydrothermal	2800−4230		1.37−2.75	Llewellyn et al.	12
microwave irradiation	3054	4443	2.01	Zhao et al.	14
microwave irradiation	3900	5900	2.30	Jhung et al.	18

where M_{EA} ($g \cdot mol^{-1}$) is the molecular weight of EA molecule; W_e (g) and W_t (g) are the amounts of adsorbents (the MIL-101 samples) at equilibrium and time t (s) respectively; W_a is the initial weight of the MIL-101; and Q_e ($mmol \cdot g^{-1}$) and Q_t ($mmol \cdot g^{-1}$) are the amount adsorbed of EA per gram of adsorbent at equilibrium and at time t (s), respectively.

3. RESULTS AND DISCUSSION

3.1. Physical Characteristics. The powder XRD pattern of the as-synthesized MIL-101 sample is given in Figure 1. Since the main peaks of the product's XRD pattern matched well with that of the MIL-101 published previously,[10] it confirmed that the product was MIL-101. In addition, the well-resolved peaks shown in Figure 1 implied the high crystallinity of the sample synthesized in this work. The nitrogen adsorption and desorption isotherms of the MIL-101 sample are shown in Figure 2. It was visible clearly that the adsorption isotherm presented a typical type-I profile with secondary uptakes, which was characteristic of the presence of the two kinds of microporous windows.[10] The textural properties of the MIL-101 sample prepared in this work and other works are listed in Table 1. The data in Table 1 indicated that the MIL-101 sample synthesized in this work had an extra-high BET specific surface area and a very high total pore volume, 3446 $m^2 \cdot g^{-1}$, and 1.75 $cm^3 \cdot g^{-1}$ separately. A comparison of textural parameters in Table 1 showed that there were some variations between the surface area and the pore volume results obtained in this work and those obtained in other works, which might be ascribed to the use of different synthesis methods and the presence of varying degrees of residual terephthalic acid and guest molecules.[16]

3.2. Adsorption Isotherms of EA on the MIL-101. The adsorption isotherms of EA vapor on the MIL-101 sample at different temperatures are presented in Figure 3. It could be seen that these isotherms all exhibited a typical type-I profile, which was comprised with a sharp increase in the uptake (at low EA relative pressure) and a following plateau. The maximum equilibrium amount adsorbed of EA on the MIL-101 sample was about 10.5 $mmol \cdot g^{-1}$ at 288 K and 54 mbar. It was also clearly visible that the adsorption capacity of the MIL-101 sample for EA decreases with temperature, indicating a physisorption between EA molecule and the MIL-101. Equilibrium amounts adsorbed of EA on other adsorbents such as activated carbon and zeolites have been reported. For example, Wang et al.[4] reported the maximum equilibrium amount adsorbed of EA on activated carbon was 4.72 $mmol \cdot g^{-1}$ at 298 K and 71 mbar; Gales et al.[17] reported a relatively lower adsorption capacity of activated carbon for EA, which was 3.5 $mmol \cdot g^{-1}$ at 298 K and 67 mbar. Manjare et al.[7] reported the adsorption capacity of activated carbon and molecular sieves 5A and 13X as 6.28 $mmol \cdot g^{-1}$, 3.89 $mmol \cdot g^{-1}$, and 4.94 $mmol \cdot g^{-1}$, at 318 K and 0.56 $kg \cdot m^{-3}$, respectively. It can be found that under similar experimental conditions the MIL-101 exhibits a larger adsorption capacity for EA, compared with that of activated carbon and molecular sieves 5A and 13X. This higher adsorption capacity can be attributed to the extra-large surface area and large pore volume of the MIL-101 sample. However, it should be mentioned that if MIL-101 is practiced in VOCs adsorption under actual conditions, the effect of water vapor on the adsorption of VOCs cannot be negligible. The competitive adsorption of H_2O molecules with VOCs on the MIL-101 would led to a decrease in adsorption capacity of the MIL-101 toward VOCs, which is worthy of systematical study later.

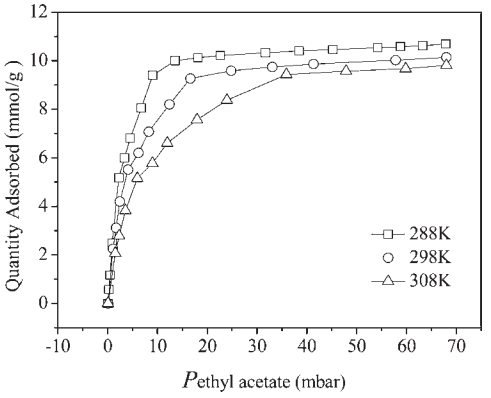

Figure 3. Adsorption isotherms of EA on the MIL-101 at (288 to 308) K.

To describe adsorption behavior of EA on the MIL-101 sample, Langmuir and Freundlich equations were applied to fit the experimental data of EA adsorption. Figure 4 gives comparisons of the experimental adsorption data and isotherm equation fits.

Table 2 lists the fitting parameters of Freundlich and Langmuir equations as well as their correlation coefficients (R^2) representing the coincidence degree between the experimental data and the isotherm equation fits. The data in Table 2 revealed that when Langmuir equation was applied the correlation coefficients were up to 0.997, which were higher than that obtained when the Freundlich equation was applied. It implied that the Langmuir model is better to fit the experimental adsorption equilibrium data of EA than Freundlich does. In addition, an examination of the data in Table 2 also informed us that the maximum equilibrium adsorption capacity (Q_m) of the sample was up to 11.3 $mmol \cdot g^{-1}$ at 288 K and decreases with an increase of temperature.

3.3. Adsorption Kinetics of EA on the MIL-101. Adsorption kinetics of EA on the MIL-101 sample has hardly been reported.

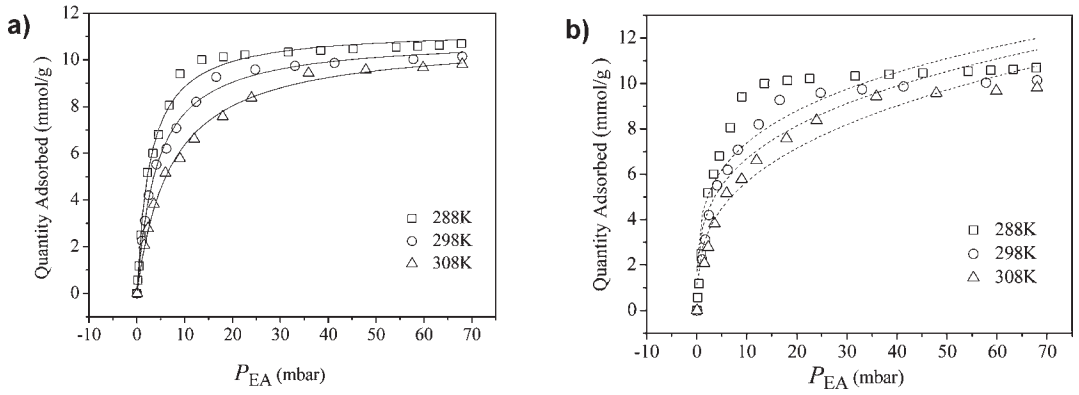

Figure 4. (a) Langmuir equation fitting of EA adsorption on the MIL-101 at (288 to 308) K; (b) Freundlich equation fitting of EA adsorption on the MIL-101 at (288 to 308) K (points: experimental data; lines: the fit curves).

Table 2. Fitting Parameters and Linear Correlation Coefficients of the Langmuir and Frendlich Equations

temperature	$Q = Q_m(bp/1 + bp)$			$Q = K_f p^n$		
K	Q_m	b	R^2	K_f	n	R^2
288	11.30	0.3610	0.9931	4.112	0.2537	0.8634
298	10.94	0.2389	0.9957	3.486	0.2826	0.9046
308	10.88	0.1404	0.9966	2.617	0.3351	0.9510

Figure 5 exhibits the kinetic curves of fractional adsorption of EA on the MIL-101 sample at 298 K and different EA vapor pressures. It could be seen that the kinetic curves of fractional adsorption of EA on the MIL-101 sample at different pressures [(2 to 5) mbar] were essentially same. This result indicated that for a given pressure range EA loading had a negligible effect on the diffusivity of EA within the MIL-101 sample. Similar phenomena can be also observed at (288 and 308) K.

Figure 6 shows the kinetic curves of fractional transient uptakes Q_t/Q_e of EA on the MIL-101 sample at different temperatures and the same EA vapor pressure. On the basis of data of these kinetic curves, the intracrystalline diffusion coefficient of EA within the MIL-101 sample can be calculated.[19] Assuming that the adsorbent is a spherical particle, the transient fractional uptakes can be described by the following equation in the region with fractional uptake Q_t/Q_e less than 70 %.[20,21]

$$\frac{Q_t}{Q_e} \cong \frac{6}{r_c}\sqrt{\frac{D_M t}{\pi}} \tag{3}$$

where D_M($cm^2 \cdot s^{-1}$) is the intracrystalline diffusion coefficient, and r_c (cm) is the particle radius. When Q_t/Q_e is plotted to $t^{1/2}$, a straight line with slope $(6/r_c)\cdot[(D_M/\pi)^{1/2}]$ is available. The diffusion time constant (D_M/r_c^2, s^{-1}) can be calculated directly from the slope, and the corresponding diffusion coefficient (D_M) can be further calculated after the average particle radius is known.

In this case, Figure 7 plots the transient fractional uptake (Q_t/Q_e) of EA adsorption versus the square root of adsorption time ($t^{1/2}$) at different temperatures. It was visible clearly that the linearity of the plots was very high, with correlation coefficients (R^2) more than 0.99, which indicated that the EA diffusion within the MIL-101 could be well-described by eq 3. From the slopes of these fitted straight lines, the diffusion time

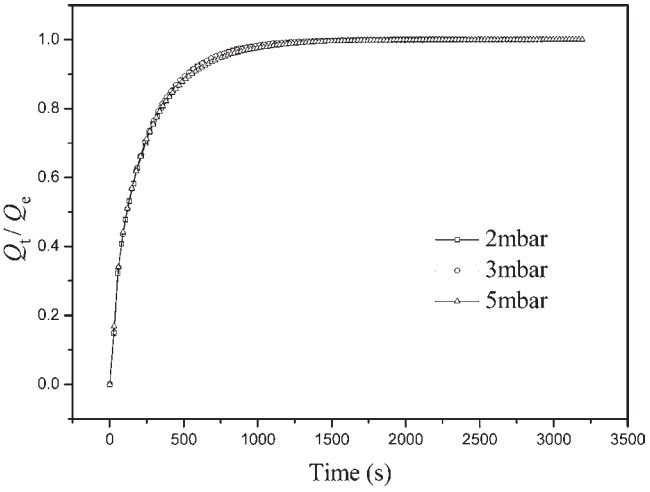

Figure 5. Fractional transient uptake of EA on the MIL-101.

constants and diffusion coefficients of EA on the MIL-101 were available, as listed in Table 3.

The data in Table 3 indicated that the diffusion coefficients (D_M) were in the range of $(1.617 \text{ to } 2.264)\cdot 10^{-10}$ $cm^2 \cdot s^{-1}$ and increased with temperature under studied conditions. Thus this implied that EA diffusion within the MIL-101 was an activated process.[22]

3.4. Estimation of the Activation Energy for Adsorption Kinetics of EA on the MIL-101. The Arrhenius equation can usually be applied to estimate adsorption/diffusion activation energy of adsorbate on an adsorbent.[23] According to the Arrhenius equation, the relationship between the diffusion coefficient (D_M) of EA and the activation energy (E_a) for EA adsorption within the MIL-101 can be expressed by the following equations:

$$D_M = A \exp(-E_a/RT) \tag{4}$$

$$\ln D_M = \ln A - (E_a/RT) \tag{5}$$

where A represents the rate coefficient, D_M ($cm^2 \cdot s^{-1}$) is the diffusion coefficient, and E_a ($kJ \cdot mol^{-1}$) is the adsorption activation energy. When ln D_M is plotted to $1/T$, a straight

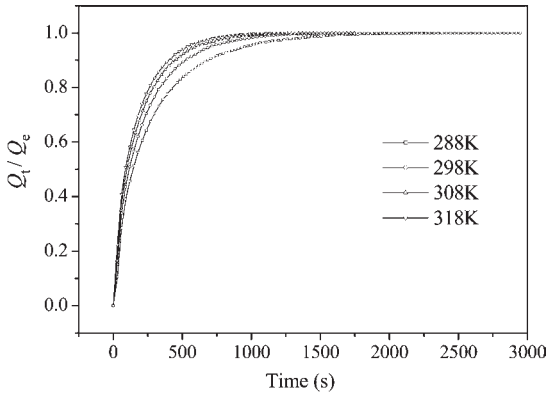

Figure 6. Fractional transient uptake of EA on the MIL-101 at different temperatures (at 3 mbar).

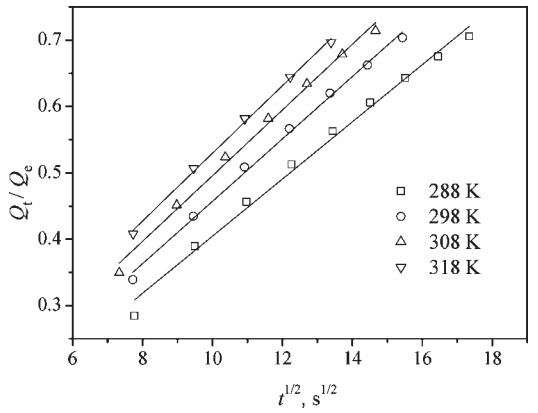

Figure 7. Plot of the fractional EA adsorption uptake (Q_t/Q_e) against the square root of adsorption time at different temperatures (at 3 mbar).

line with slope $-E_a/R$ will be yielded. From the slope of the line, the activation energy E_a can be easily found out.

The plot of ln D_M versus $1/T$ for benzene diffusing in the MIL-101 crystals is shown in Figure 8. The activation energy (E_a) of EA diffusion within the MIL-101 was calculated from the slope of this straight line, which value was about 8.361 kJ·mol^{-1}.

3.5. Estimation of the Isosteric Heat of Adsorption for EA on the MIL-101. Isosteric heat (enthalpy) of adsorption is an important parameter, and it can characterize the interaction between the adsorbate molecules and the adsorbent surfaces. The isosteric heats of adsorption can be calculated from isotherms at different temperatures by using the Clausius−Clapeyron equation, which is described as follows:

$$\ln p = -\frac{\Delta H}{RT} + C \qquad (6)$$

where ΔH (kJ·mol^{-1}) is the isosteric heat of adsorption at specific EA loading and temperature on the MIL-101. The isotherms of EA on the MIL-101 at (298, 308, 318, and 328) K were used to calculate the heat of adsorption. First, the EA isotherms were converted to EA adsorption isosteres, a plot of ln p versus $1/T$ at a given adsorption amount of EA. After ln p was plotted to $1/T$, a straight line with a slope $-\Delta H/R$ was yielded. Finally, ΔH could be calculated directly from the slope $-\Delta H/R$ of the plotted straight line.

Table 3. EA Diffusion Constants and Diffusion Coefficient within the MIL-101 Measured in This Work

temperature (K)	288	298	308	318
D_M (10^{-10} cm^2·s^{-1})	1.617	1.927	2.137	2.264
R^2	0.9909	0.9958	0.9932	0.9970

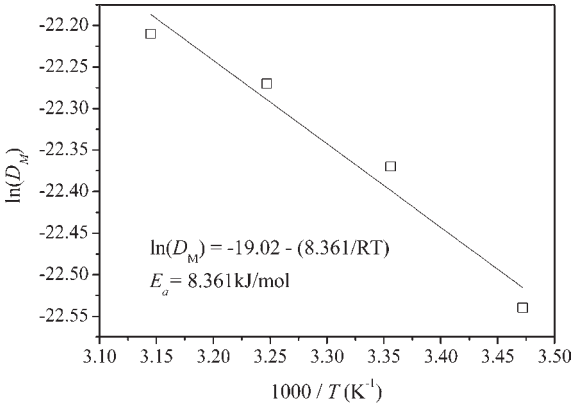

Figure 8. Arrhenius plot of EA diffusivity in the MIL-101 crystals.

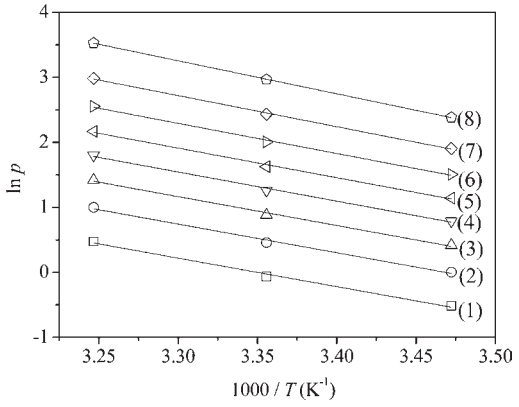

Figure 9. ln p versus $1/T$ for the estimation of isosteric adsorption heats of EA on the MIL-101: (1) Q = 2 mmol·g^{-1}; (2) Q = 3 mmol·g^{-1}; (3) Q = 4 mmol·g^{-1}; (4) Q = 5 mmol·g^{-1}; (5) Q = 6 mmol·g^{-1}; (6) Q = 7 mmol·g^{-1}; (5) Q = 8 mmol·g^{-1}; (6) Q = 9 mmol·g^{-1}.

Figure 9 exhibits a series of plots of ln p versus $1/T$ at different amounts adsorbed of EA. From the slope of the plotted straight lines, the isosteric heats (ΔH) of EA adsorption on the MIL-101 under various EA loadings were available. After that the dependence of the isosteric heat on the amounts adsorbed of EA over the MIL-101 was obtained, as shown in Figure 10. It exhibits an increasing trend of the isosteric heats of adsorption with an increase in the amount adsorbed of EA. The data in Figure 10 indicated that the isosteric heats of EA adsorption were within the range of (36.48 to 42.25) kJ·mol^{-1} and increased slighted with an increase of the amount adsorbed of EA on the MIL-101. It has been proved that for a slightly heterogeneous surface the isosteric heat of adsorption can be expressed as an increasing function of the surface coverage or the amount of adsorbed molecules on the surface of adsorbent.[24] Thus, in this work this increasing trend of the isosteric adsorption heats with an increase in the amount adsorbed of EA can be ascribed to the existence of

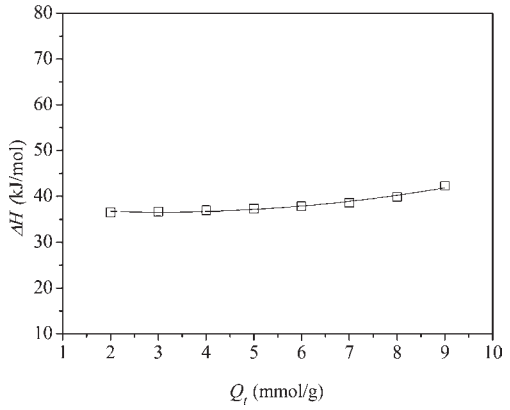

Figure 10. Dependence of isosteric adsorption heat on the amounts adsorbed of EA over the MIL-101.

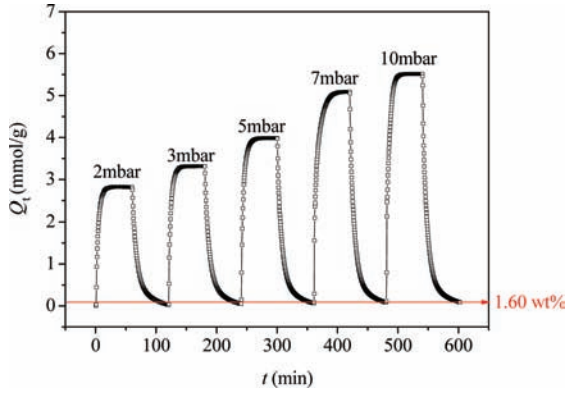

Figure 11. Five consecutive cycles of EA adsorption−desorption on the MIL-101 at 298 K.

favorable lateral interactions between EA molecules on the slightly heterogeneous surfaces of the MIL-101 sample.

3.6. Multiple Cycles of EA Adsorption−Desorption on the MIL-101. Multiple adsorption−desorption cycles were conducted at 298 K to examine the reversibility of EA adsorption on the MIL-101. During the experiment, adsorption was performed separately at (2, 3, 5, 7, and 10) mbar, and desorption was performed at 0.05 mbar. Figure 11 exhibits the five EA adsorption−desorption cycles. It was visible clearly that, for adsorption processes, the working adsorption capacities of the MIL-101 for EA increased with an increase of adsorption operation pressure, and for desorption processes at 0.05 mbar, the amounts adsorbed of EA decreased sharply to very low content, about (1.0 to 1.60) wt % of residual EA on the sample. It suggests that more than 98.4 % of EA adsorbed on the sample could be desorbed. In the other words, the application of vacuum desorption was effective in stripping adsorbed EA from the MIL-101and thus allowed it restore 98.4 % of its adsorption capacity for EA. Since after five adsorption−desorption cycles, the efficiency of EA desorption on the MIL-101 was still kept up to 98.4 %, it could be concluded that adsorption and desorption properties of the MIL-101 sample for EA were stable or repeatable.

4. CONCLUSIONS

The MIL-101 sample synthesized in this work shows an extra-high surface area of 5014 $m^2 \cdot g^{-1}$ (Langmuir). The isotherms of EA on the MIL-101 sample can be fitted favorably by using the Langmuir equation. The adsorption capacity of the MIL-101 for EA is up to 10.5 $mmol \cdot g^{-1}$ at 288 K and 54 mbar. The diffusion of EA within the MIL-101 crystals is an activated process with diffusivity in the range of (1.617 to 2.264)$\cdot 10^{-10}$ $cm^2 \cdot s^{-1}$ at (288 to 318) K, and the diffusion activation energy of EA is 8.361 $kJ \cdot mol^{-1}$. The isosteric heat of EA adsorption on the MIL-101 is within the range of (36.48 to 42.25) $kJ \cdot mol^{-1}$. The isosteric adsorption heat increased slightly with the amounts adsorbed of EA due to the existence of favorable lateral interactions between EA molecules on the surfaces of the MIL-101 sample. Experiments of consecutive cycles of EA adsorption−desorption show that the adsorption of EA on the MIL-101 is a highly reversible process. More than 98.4 % of EA adsorbed on the sample can be desorbed. In the other words, the desorption efficiency of EA was up to 98.4 %. The EA adsorption and desorption properties of the sample MIL-101 are stable or repeatable.

AUTHOR INFORMATION

Corresponding Author

*E-mail: cezhli@scut.edu.cn.

Funding Sources

This work was supported by National Natural Science Foundation of China (No. 20936001), the State Key Laboratory of Subtropical Building Science, South China University of Technology (Grant C710090Z), and Pulp & Paper Engineering State Key Laboratory for financial support.

REFERENCES

(1) Manjare, S. D.; Ghoshal, A. K. Studies on dynamic adsorption behaviour of ethyl acetate on molecular sieves. *Can. J. Chem. Eng.* **2005**, *83*, 232–241.

(2) Li, Y. X.; Zhang, Y. C. Removal of trace amount of benzene from CO_2 by adsorption with modified activated carbon. *Huagong Xuebao (Chin. Ed.)* **2009**, *60* (6), 1494–1499.

(3) Yamauchi, H.; Kodama, A.; Hirose, T.; Okano, H.; Yamada, K. Performance of VOC Abatement by Thermal Swing Honeycomb Rotor Adsorbers. *Ind. Eng. Chem. Res.* **2007**, *46*, 4316.

(4) Wang, C. M.; Chung, T. W.; Huang, C. M.; Wu, H. Adsorption Equilibria of Acetate Compounds on Activated Carbon, Silica Gel, and 13X Zeolite. *J. Chem. Eng. Data* **2005**, *50*, 811–816.

(5) Manjare, S. D.; Ghoshal, A. K. Studies on adsorption of ethyl acetate vapor on activated carbon. *Ind. Eng. Chem. Res.* **2006**, *45* (19), 6563–6569.

(6) Manjare, S. D.; Ghoshal, A. K. Adsorption equilibrium studies for ethyl acetate vapor and E-Merck 13X molecular sieve system. *Sep. Purif. Technol.* **2006**, *51* (2), 118–125.

(7) Manjare, S. D.; Ghoshal, A. K. Comparison of adsorption of ethyl acetate on activated carbon and molecular sieves 5A and 13X. *J. Chem. Eng. Data* **2006**, *51* (4), 1185–1189.

(8) Cavazzini, A.; Nadalini, G.; Costa, V.; Dondi, F. Heterogeneity of adsorption mechanisms in chiral normal-phase liquid chromatography. 2-Propanol and ethyl acetate adsorption equilibria. *J. Chromatogr., A* **2007**, *1143* (1−2), 134–142.

(9) Li, Y. X.; Chen, J. Y.; Sun, Y. H. Adsorption of multicomponent volatile organic compounds on semi-coke. *Carbon* **2008**, *46* (6), 858–863.

(10) Ferey, G.; Mellot-Draznieks, C.; Serre, C.; Millange, F.; Dutour, J.; Surble, S.; Margiolaki, I. A Chromium Terephthalate-Based Solid with Unusually Large Pore Volumes and Surface Area. *Science* **2005**, *309*, 2040.

(11) Küsgens, P.; Rose, M.; Senkovska, I.; Fröde, H.; Henschel, A.; Siegle, S.; Kaskel, S. Characterization of metal-organic frameworks by water adsorption. *Microporous Mesoporous Mater.* **2009**, *120*, 325–330.

(12) Llewellyn, P. L.; Bourrelly, S.; Serre, C.; Vimont, A.; Daturi, M.; Hamon, L.; De Weireld, G.; Chang, J. S.; Hong, D. Y.; Hwang, Y. K.; Jhung, S. H.; Ferey, G. High Uptakes of CO_2 and CH_4 in Mesoporous Metal-Organic Frameworks MIL-100 and MIL-101. *Langmuir* **2008**, *24*, 7245.

(13) Hamon, L.; Serre, C.; Devic, T.; Loiseau, T.; Millange, F.; Ferey, G.; De Weireld, G. Comparative Study of Hydrogen Sulfide Adsorption in the MIL-53(Al,Cr,Fe), MIL-47(V), MIL-100(Cr), and MIL-101(Cr) Metal-Organic Frameworks at Room Temperature. *J. Am. Chem. Soc.* **2009**, *131*, 8775–8777.

(14) Zhao, Z. X.; Li, X. M.; Huang, S. S.; Xia, Q. B.; Li, Zh. Adsorption and Diffusion of Benzene on Chromium-Based Metal Organic Framework MIL-101 Synthesized by Microwave Irradiation. *Ind. Eng. Chem. Res.* **2011**, *50* (4), 2254–2261.

(15) Hong, D. Y.; Hwang, Y. K.; Serre, C.; Ferey, G.; Chang, J. S. Porous Chromium Terephthalate MIL-101 with Coordinatively Unsaturated Sites: Surface, Functionalization, Encapsulation, Sorption and Catalysis. *Adv. Funct. Mater.* **2009**, *19*, 1537–1552.

(16) Chowdhury, P.; Bikkina, C.; Gumma, S. Gas Adsorption Properties of the Chromium-Based Metal Organic Framework MIL-101. *J. Phys. Chem. C* **2009**, *113*, 6616.

(17) Gales, L.; Mendes, A.; Costa, C. Hysteresis in the cyclic adsorption of acetone, ethanol and ethyl acetate on activated carbon. *Carbon* **2000**, *38*, 1083–1088.

(18) Jhung, S. H.; Lee, J. H.; Yoon, J. W.; Serre, C.; Ferey, G.; Chang, J. S. Microwave Synthesis of Chromium Terephthalate MIL-101 and its Benzene Sorption Ability. *Adv. Mater.* **2007**, *19*, 121.

(19) Zhao, Z. X.; Li, Z.; Lin, Y. S. Adsorption and Diffusion of Carbon Dioxide on Metal-Organic Framework (MOF-5). *Ind. Eng. Chem. Res.* **2009**, *48*, 10015.

(20) Yang, R. T. *Gas Separation by Adsorption Processes*; Imperial College Press: London, 1997.

(21) Zhang, Z.; Huang, S.; Xian, S.; Xi, H.; Li, Z. Adsorption Equilibrium and Kinetics of CO_2 on Chromium Terephthalate MIL-101. *Energy Fuels* **2011**, *25*, 835–842.

(22) Skoulidas, A. I. Molecular Dynamics Simulations of Gas Diffusion in Metal-Organic Frameworks: Argon in CuBTC. *J. Am. Chem. Soc.* **2004**, *126*, 1356.

(23) Zhang, Z.; Zhang, W.; Chen, X.; Xia, Q.; Li, Z. Adsorption of CO_2 on Zeolite 13X and Activated Carbon with High Surface Area. *Sep. Sci. Technol.* **2010**, *45*, 710–719.

(24) Al-Muhtaseb, S. A.; Ritter, J. A. Roles of Surface Heterogeneity and Lateral Interactions on the Isosteric Heat of Adsorption and Adsorbed Phase Heat Capacity. *J. Phys. Chem. B* **1999**, *103*, 2467–2479.